International Journal of
INTELLIGENT SYSTEMS AND APPLICATIONS IN ENGINEERING
ISSN:2147-6799 www.ijisae.org Original Research Paper

A Novel Framework for Brain Tumor Segmentation using Neuro Trypetidae Fruit Fly-Based UNet

A. Vinisha[1,2], Ravi Boda[3]

Submitted: 28/06/2023 **Revised**: 08/08/2023 **Accepted**: 27/08/2023

Abstract: Most challenging tasks associated with medical image processing involve segmenting and analyzing complex images, such as brain images. Additionally, MRI scans are frequently used to forecast many brain ailments; if the scans are complicated, the disease forecasting precision is relatively low. The current study has designed an approach to deal with this issue.to create a cutting-edge Trypetidae fruit fly-based UNet (TFFbU) system to precisely detect the tumour. Additionally, the UNet pooling module increased the Trypetidae fruit fly's fitness. That has typically produced the best outcomes. In the beginning, the system was trained using the standard datasets that are collected from the internet. As a result, the training errors are eliminated in the TFFbU's primary layer before the data has been cleaned of errors, which is then used to detect and segment tumours in the UNet dense layer. Lastly, the suggested model is run in MATLAB, and the effectiveness of the developed TFFbU. The model is estimated with various parameters like accuracy, recall, precision, Dice, and Jaccard. Additionally, the projected innovative TFFbU model has the capacity to segment and predict various tumour varieties.

Keywords: *MRI brain tumour pictures, feature extraction, tumour segmentation, tumour tracking, Dice and Jaccard, Trypetidae fruit fly optimization, and UNet deep learning*

1. Introduction

Tumours are the term for an abnormal growth of cells in the human body; brain tumours can be fatal. Additionally, a more sophisticated image processing program is needed to find the brain tumour. The brain, which serves as the body's central nervous system, is made up of a large number of cooperative neurons.[3] In the past, a number of tumour segmentation strategies, such as high and low-level glioma, have been used.[4] But it has been challenging to segment the brain tumours due to the intricacy and variety of the brain picture from person to person. The brain tissues may also be impacted by the quickly expanding tumours in the brain. The identification of specific sub-regions inside a brain tumor is a crucial step in a variety of medical operations, including the monitoring of the growth of a tumor, surgical procedures, radiation, and other therapies. In addition, defining the border or sub-region of the brain before attempting to segment the tumor makes it far more difficult to do so with a high level of exactness. [7] It describes the fundamental brain tumour segmentation system. Figure 1 For that, boundary masking images or ground truth photos were used. The damaged area was then identified during testing by comparing the test samples to the ground truth samples.[9] The manual method of analyzing and monitoring the brain tumour, however, is challenging and has taken longer.[10] In addition, BraTS data, which contains 660–2000 pictures, is the most commonly used data for predicting brain tumours.[11] Additionally, a lot of approaches have addressed how challenging it is to validate training and testing in the BraTS database. Additionally, soft computing approaches like Machine Learning (ML) and Deep Learning (DL) methods are successfully applied for segmenting brain tumours.[13]The best result has been achieved in this while taking the ML into consideration by using DL.[14] On the other hand, numerous patients with aberrant brain cells participated in medical conferences to test the validity of the system that was presented.[15] These patients' MRIs were obtained by scanning, and the severity of the aberrant cell was assessed using the neurological model.[16] In the past, many techniques, such as the remaining neural framework, the level set approach, the fuzzy with Boltzmann notion, and others, were used in order to segment brain tumors. However, the issues are still there since the method needs to take additional time to trace the affected region and has a propensity to obtain a very low exactness rate of segmentation when analyzing pictures that have a slight alteration. Both of these issues make it difficult for the method to be used. As a result, the primary focus of the work being done for this project has been on the creation of an innovative and improved DL approach that will allow for the most accurate tracing of impacted regions and the most accurate segmentation results.

[1]*Research Scholar, Department of Electronics and Communication Engineering, Koneru Lakshmiah Education Foundation, Hyderabad campus, Telangana 500075, India.*
[2]*Assistant Professor, Department of Electronics and Communication Engineering, Guru Nanak Institutions Technical campus, Ibrahimpatnam R.R Dist,Telangana 501506, India.*
[3]*Corresponding Author, Department of Electronics and Communication Engineering, Koneru Lakshmiah Education Foundation, Hyderabad campus, Telangana 500075, India.*

The following is the structure of the research work that has been presented: Following the presentation of examples of similar works in Section 2, which is followed by the presentation of the system model and the problem description in Section 3, there is a discussion of the offered scheme in Section 4, which is followed by illustrations of the model's outcomes in Section 5, and then a conclusion is presented in Section 6.

2. Related works

Following is a discussion of a few recent types of literature on segmenting and predicting brain tumours:

Zhou et al.[17] created three-dimensional residual neural frameworks in the GPU environment for the automatic segmentation of brain tumours. The resilience of the designed system has been measured using the BRATS 2018 dataset. Finally, it now has the highest rate of segmentation accuracy. However, it took the largest amount of time to identify the tumor's segment from the images.

The most well-known method to identify and assess the affected area in medical applications is by looking for tumours on the basis of MRI images. Lei et al. used a level set technique to determine the optimal exactness score for the segmentation of brain tumours.[18] The experiment shows that the suggested system improved segmentation accuracy by 96%. However, more resources were needed for the implementation process.

The brain tumour segmentation method was created by Khosravanian et al.[19] using a fuzzy with Boltzmann idea. A gradient reconstruction method was also used to produce the multiscale supervised region. Additionally, the BraTS2017 database is used to assess how effective the designed method is. The recorder's quick execution time, minimal noise, and great accuracy were its last successes. But creating the discussed model is challenging.

Due to their requirements, segmentation of brain tumours is the most popular issue in medicine. In order to extract the tumor cell from the MRI images of the brain, Zhang et al. [20] developed the cross-modality, which is based on deep features. Using the ground truth images, the cancer cells in the MRI of the patient's brain are followed here. Finally, the created model now provides the highest level of tumour segmentation accuracy. The work will take longer to complete if the dataset is too big, though.

Tiwari et al.[21] have performed a thorough analysis of brain tumour extraction methods to understand the benefits and drawbacks of each employed methodology. Graphs and table graphics were then used to estimate each performance. The models in this review include ML, DL, and heuristic methods. Finally, some suggestions were made to improve the segmentation procedure. Following is a description of the suggested model's main process:

• In the beginning, the MRI brain images are gathered from the usual sources and analyzed by the system.

•As a result, an innovative TFFbU was created with the necessary packages and functions, including pre-processing, tracking, and segmentation capabilities.

•The pre-processing layer first removes the errors from the training databases.

•In order to track and segment tumours, the pre-processed data is added to the UNet dense layer.

• Finally, the accuracy, recall, execution time, F-measure, and precision of tracking and segmentation performance are assessed.

When compared to other organs, the neuron components that make up the brain are the smallest, which makes it challenging to conduct an investigation into the specific qualities of a brain cell. [22] Additionally, each person has a unique set of brain structures. The analysis of the literature confirmed that many methodologies had significantly suffered as a result of data complexity. In order to achieve the best outcomes, adjusting the neural model parameters has been attempted.

In a variety of medical applications, the model UNet is used for the purpose of extracting the diseased component from previously learned data. Here, the noisy data has produced a score for exactness that is lower. The lengthy execution period is another one of this Conventional UNet model's main drawbacks. When the size of the data rises during processing, the UNet may slow down the operation, which tends to report a lengthy processing time for the function. Additionally, Figure 2 details the acknowledged issue with the system model. Therefore, the goal of the current effort was to create an efficient module for the UNet architecture to fine-tune the process.

3. Proposed methodology

The necessary brain MRI data is first gathered from the usual sources and trained on the MATLAB system before a fresh TFFbU was created with the necessary parameters. The pre-processing layer then corrects the flaws in the trained images, and the error-free data is then transferred into the classification layer. Two of the tasks that are finished at the classification layer are segmentation and tracking. When Trypetidae fruit fly fitness was used to improve the tracking and segmentation algorithm, the best results were achieved. The recommended architecture is shown in Figure 3. Ultimately, the optimal outcome is given once the generated model's performance is confirmed using a number of measures, such as accuracy, Dice, and Jackccard.

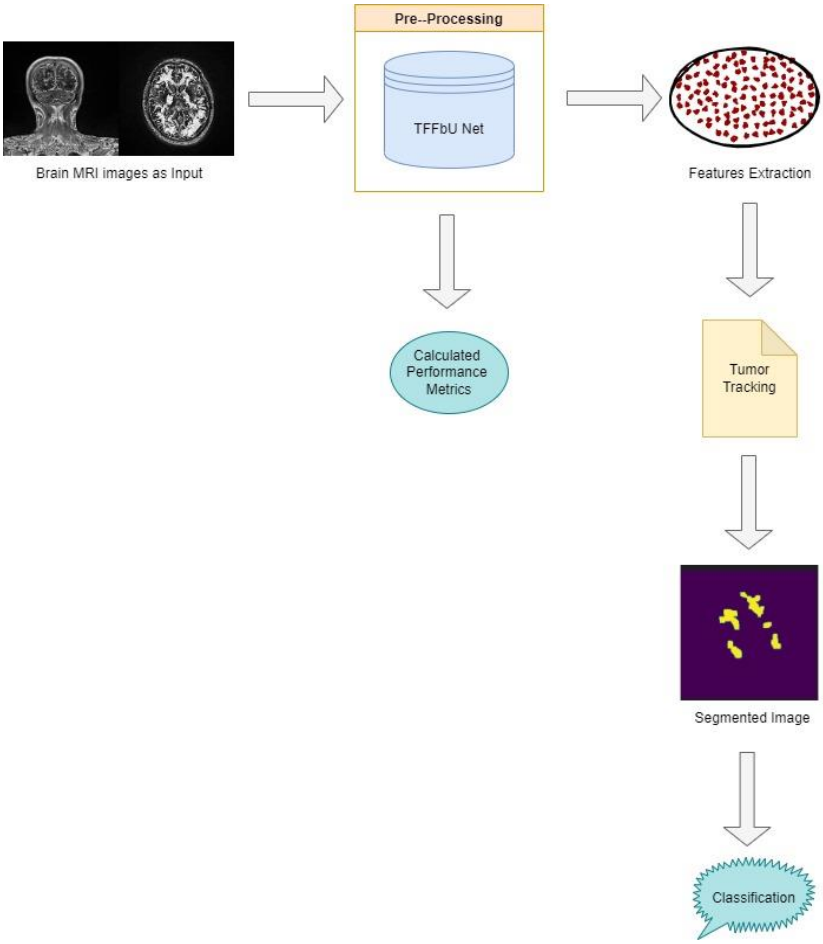

Fig 1. shows Proposed Methodology

Data Set

The medical database is compiled from the well-known open-source website Kaggle and includes a variety of medical data, including MRI, X-ray, and scan results, among other things. The algorithm is trained using a variety of brain tumour MRI data. Furthermore, this dataset includes 2500 photos of the four different tumour types: metastatic, astrocytic, meningioma, and pediatric.

TFFbU layer Design

The Brain Tumor detection system with the integration of UNet and Trypetidae fruit fly (TFF) fitness has been provided in the current research. Here, TFF fitness has been included to the UNet's classification module. Equation (1) first discusses the training procedure for brain MRI images.

$$TFF(db) = \alpha^{*}(1,2,3,\dots n) \qquad (1)$$

The TFFbU model that was envisioned has a total of six levels, with the pre-processing, classification, entropy weight activation, and optimization layers being some of the layers included. There are main and sub neurons in the TFFbU's layers, which are depicted in Figure 2. Once the data has been trained on the model, these neurons are used to partition and distribute the data across a large number of sub neurons. The number of sub neurons depends on the size of the database. The proposed TFFbU is produced using Fruit fly fitness [23] and UNet model [24], which is how the best result was attained in this particular instance by fine-tuning the classification parameter of the UNet model. This is how the suggested TFFbU is constructed.

Pre-processing

To increase the accuracy of predicting disease severity and reduce disease complexity, the pre-processing function was used. All computer vision applications must use the function pre-processing to achieve the best results.

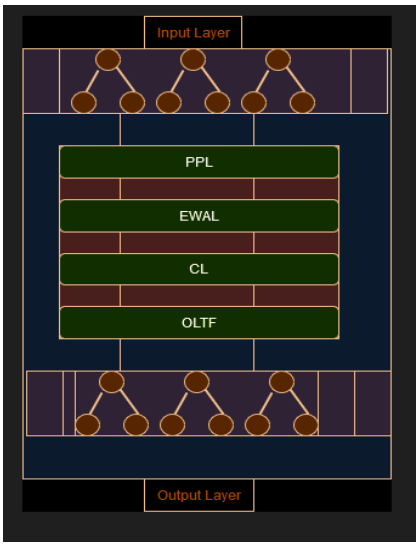

Fig 2. Design of TFFbU layers

The pre-processing step seeks to remove training faults visible in the trained MRI images. The pre-processing model is added to the secondary layer of TFFbU in this study.

$$\frac{\Sigma_{\alpha^*=1}^{n}\left\{\alpha^*_{(data,a)}=\alpha^*_{(data,a)}\right\}data}{\Sigma_{data=1}^{n}\left\{\alpha^*_{(data,a)}=\alpha^*_{(data,a)}\right\}^{l}} = N_e\left(\alpha^*_{data,a}\right) \qquad (2)$$

Each image in the training set is represented as a, and the noisy contents are represented as $N_e(\alpha^*_{data,a})$, where α^*_{data} is the trained BT MRI image. Using the error filtering algorithm described in Equation (2), the presence of noise in the data was demonstrated.

$$E_f = \alpha^*_{data} - N_e\left(\alpha^*_{data,a}\right) = \alpha_{data} \qquad (3)$$

The variable used to filter errors is designated here as E_f. As a result, Equation (3) performed the error filtering process. The error-cleared data were used for the subsequent phase after the error-free data had been retrieved and represented as α_{data}.

Feature Extraction

Using pixel analysis, the features of the training brain MRI images were retrieved. The primary driver behind feature extraction is the unjustified dimensionality reduction to achieve successful illness segmentation and prediction. The histogram model also recognizes the components that are present in the images. here, α^* is widely used brain database and $\alpha^*(1,2,3,\ldots.n)$ are brain MRI scans, and Equation (4) was used to carry out the pixel tracing operation. Additionally, the feature channel activation parameter is indicated as $fc_{ac}(x)$ and the variable used to evaluate pixels was identified as $P(\alpha^*)$..

$$P(\alpha^*) = \exp\left(fc_{ac}(x)\right)/\left(\sum_{ac1}^{ac}\exp\left(fc_{ac}(x)\right)\right) \qquad (4)$$

The pixel tracking process is started after the pre-processing module to look at each MRI picture's pixel range. This indicates that there are *ac* required classes. Equation (5) provides the weight calculation process after the weight activation function was initiated after the pixel's location in the images. Here, l_f stands for layer frequency, ω_b for weight balancing parameter, $\tau_\delta$and β for the threshold pixel value of brain characteristics.

$$w(B) = \omega_b(B) + \tau_\delta\left(-\frac{(l_{f1}(B)+l_{f2}(B))^2}{\beta^2}\right) \qquad (5)$$

After that, Equation (6) is used to extract the features from the trained brain MRI. Here, the present features in the trained set are identified as γ^*, and the feature mining parameter is indicated as γ_e. The wp here represents the brain feature pixel, which is used to extract the current features from the test images. Every picture also includes thorough and pertinent data. So it's crucial to extract the valuable characteristic in order to lessen algorithm complexity. As a result, the dataset was trained using raw image data and brain features. During the testing process, different brain features were compared with each picture. The features that were successfully matched were then retrieved.

$$\gamma_e = \gamma^*(B) + (\tau_\delta + \beta) \qquad (6)$$

To monitor the tumor area quickly, feature extraction is a necessary function. After all of the features from the trained MRI images have been followed and segmentation has been completed, the GTI function is then enabled to identify the tumor cell. This allows the GTI function to recognize the tumor cell.

Segmentation Process

Equation (7) handles the tracking and segmentation procedure because the impacted region was tracked and segmented following the feature extraction function. The aberrant cell characteristic identified in this instance is φ_f.

$$\mathbb{s}_{\mathbb{p}} = \gamma^*(B) + \varphi_f \qquad (7)$$

In addition, the Ground Truth Image (GTI), which was obtained with the help of the ML animation tool, is matched in order to carry out the function of segmentation. As a result of this, the system is trained using both GTI and MRI brain images. Following this, the characteristics included in the MRI images are retrieved utilizing the information contained in the GTI images. After that, the segmentation process is carried out.

ALGORITHM 1. TFFbU

start

{

Int $\alpha = (1,2,3, \ldots n)$

// brain db initialisation

Pre-processing Module

{

Int E_f; //initialising error filtering parameter

$E_f \dashrightarrow \alpha_{data}$

// the error was filtered using equation (3)

}

Feature extraction ()

{

Analyse P(db)

// the pixels of every image is analysed

Layers weight of (objects) = $w(B)$

Threshold-set = (τ_δ, β)

// Threshold values have been set in the trained BT images to track a particular object.

}

Segmentation process()

{

$\mathbb{S}_{\mathbb{p}} \dashrightarrow \varphi_f$

// aberrant cell feature identification

Tumor tracking ()

If ($\varphi_f = p < 0.001$) // here p is the variance

{

pediatric

}

If (tumor_dia < 2 cm) // tumor_dia represents tumor diiameter

{

meningioma

}

If (tumor_dia = 10 mm)

{

```
            metastatic
        }
    If ( tumor_dia >= 6 cm)
        {
            astrocytic
        }
    // by evaluating these threshold values segmentation is performed
}
Stop
```

Algorithm 1 describes in detail the projected FFbU model's methodology. Additionally, a unique FFbU that can segment the various illness brain tumour types was proposed in the current research publication. The segmental and expected diseases in this case include meningioma, astrocytic, metastatic, and pediatric. The brain cells in this case have been impacted by the BT diseases listed, as well as the brain from tumours such meningiomas. spinal cord cell in a cell. Additionally, the fitness layer was taught to locate various tumours using the specific behaviours of the tumour. It is beneficial to monitor and divide the impacted the training MRI BT picture region. Consequently, Algorithm 1 illustrates the whole function.

4. Results and Discussion

The MATLAB R2018b program, operating in a Windows 10 environment, is used to implement the anticipated innovative TFFbU model. The relevant data is first obtained from the default Kaggle citation, and it is then imported into the MATLAB system. TFFbU, a new model to track the damaged region and extract the tumor from brain MRI, was developed with the required parameters. To test the effectiveness of the TFFbU system, a number of images of BT illnesses are captured. The developed model is then applied to those images. We tested the resilience in several settings by selecting illnesses related to meningioma, metastatic, intracranial, and pediatrics. The system is trained with a set of MRI and GTI inputs for each condition, and the tumor is found by comparing the GTI. Tumors are segmented using the developed model. With the use of variance and tumor size, the classification layer fitness module sets the tumor size and conflicts. It provide more information on the various BT segmentations and the data that support them. Less than 0.001 variance, less than 2 cm in diameter, and 10 mm are the ranges that were taught to segment the BT. For an astrocytic tumor, the size must be less than or equal to 6 cm. All Bt are recognized by training the illness range statistics and divided. As a result, the created model is a multi-BT segmentation model with great accuracy.

Performance Analysis

By assessing the important parameters with various sets of data, the robustness and functionality of the developed TFFbU model are examined. As a result, metrics including Dice, precision, accuracy, Jaccard, and specificity recall were evaluated for varying amounts of data and have returned the best performance results for each metric. To comprehend the effectiveness and scope of the trained and test data, the confusion matrix was validated. The projected classes in this case are determined as 0 and 1, and the segmentation effectiveness was diagonally tested. In this case, the rounded value of the dice is 0.99, and loss is represented by 0.01. The recorded Jaccard value is 0.98, while its loss is 0.02 at the same time.

Segmentation Results

The approach is regarded as the best model because it produced the highest accuracy in a brief amount of time. With regard to each distinct ailment, the segmentation period was computed using unique disease data counts.

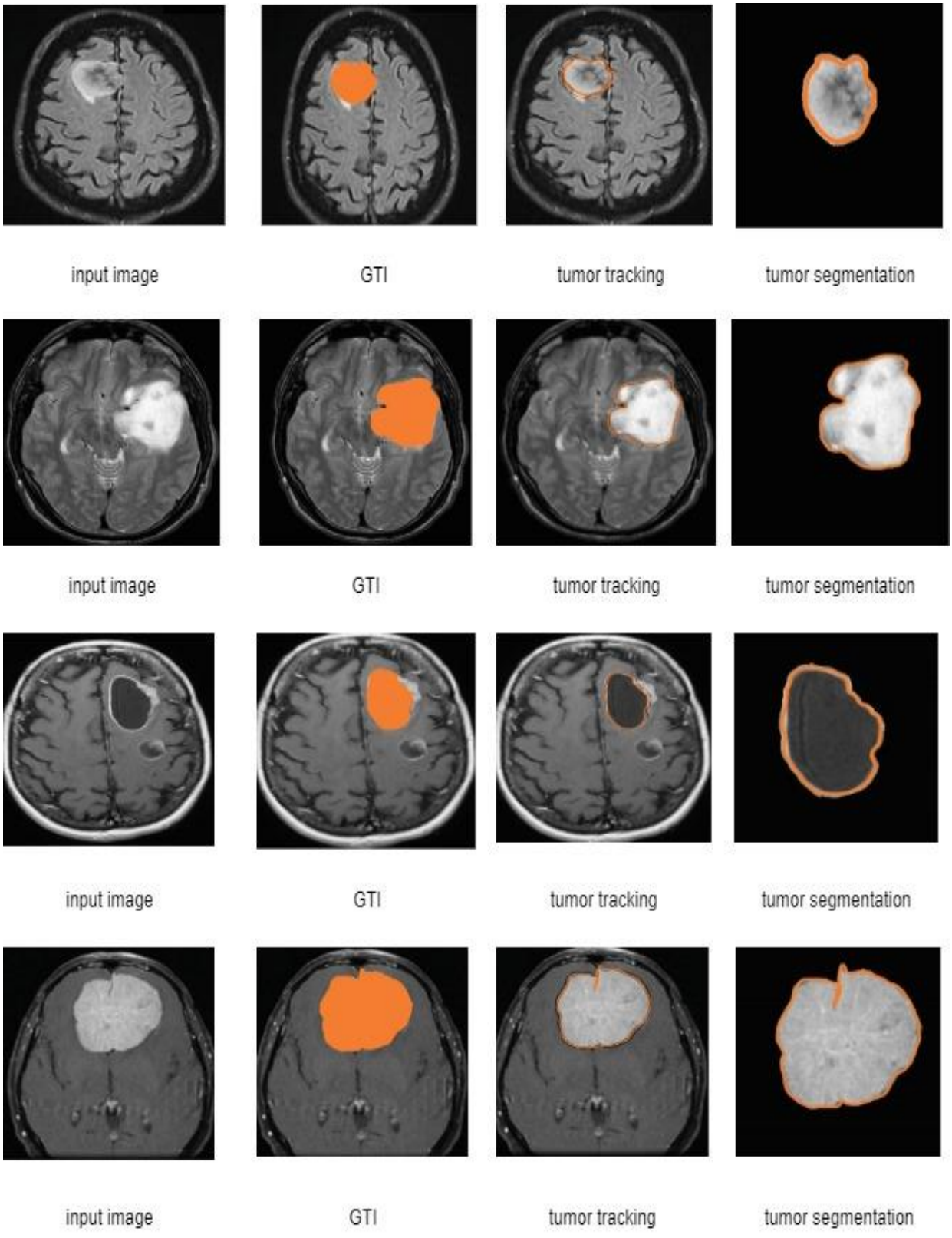

Fig 3. shows Paediatric, Astrocytic, Metastatic and Meningioma

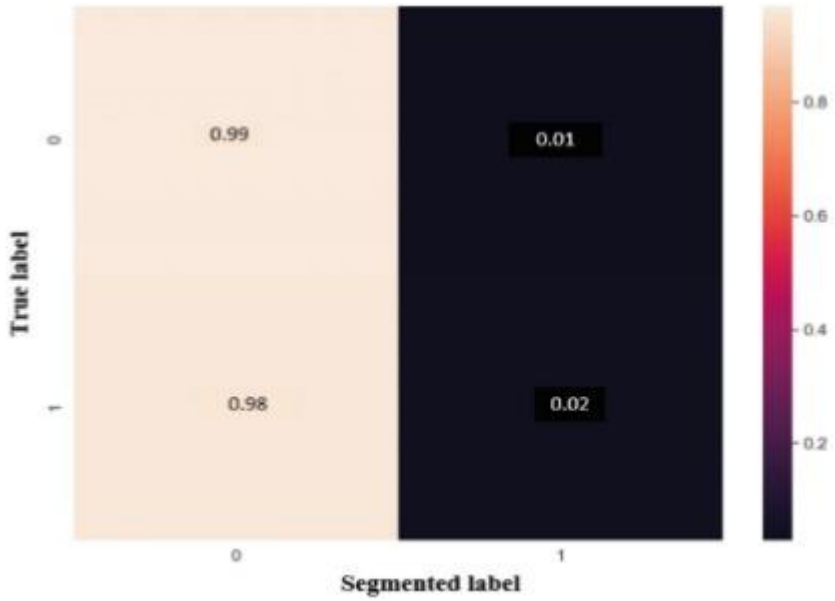

Fig 4. shows Confusion Matrix

2500 BT MRI pictures were used in this study to train the system, and the dataset includes cases of meningioma, astrocytic BT disease, metastatic BT illness, and pediatric BT disease. To evaluate the performance of the TFFbU, 2500 data are divided into 80% training and 20% testing data. Additionally, there are 600 total images for meningioma BT MRI, 600 for astrocytic BT MRI, 600 for metastatic BT MRI, and 600 for pediatric BT MRI.We used 80% training and 20% testing for each BT illness dataset. Figure 4 gives a detailed analysis of segmentation time. The dataset is trained independently for each disease in order to evaluate the performance of the proposed algorithm's flexibility score. Consequently, the training to testing ratio for each set of illness picture data is in the range of 80:20.

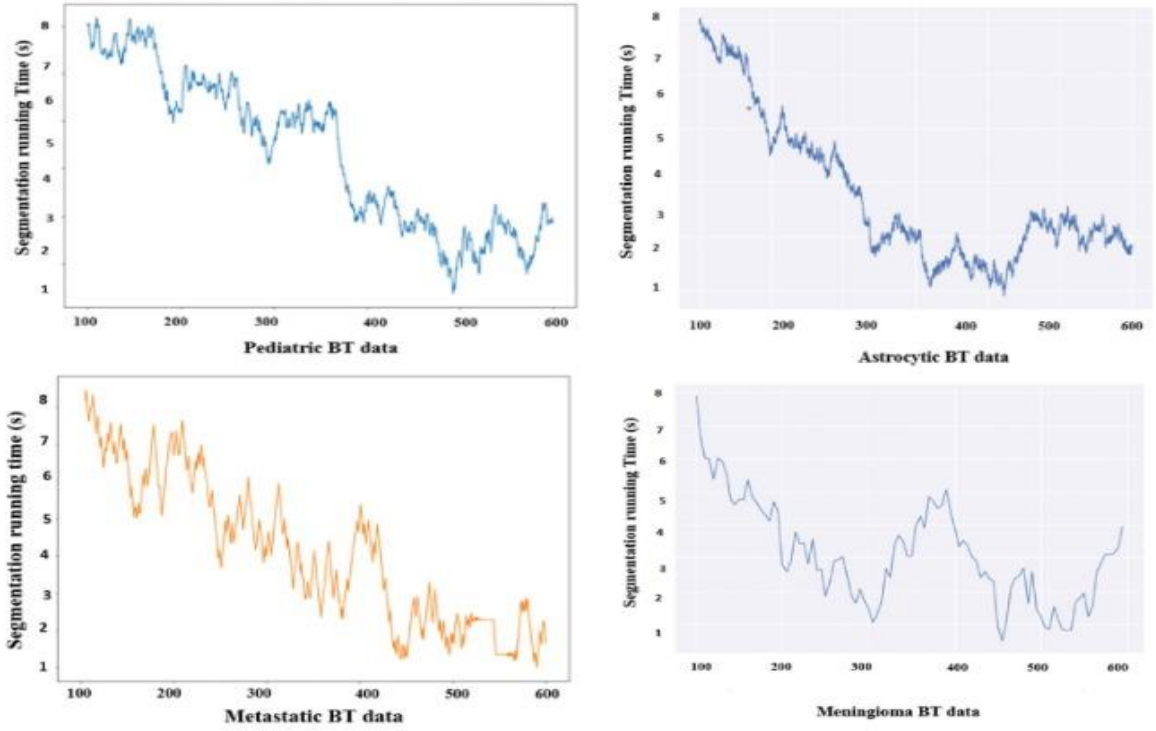

Fig 5 shows Assesment of Segmentation Time

Accuracy and Precision

The accuracy of the tumour segmentation score is measured with the use of the trained MRI brain database. This metric is a statistic that may be used in any application involving machine learning or image processing in order to evaluate the robustness rate and keep track of the complexity score of the model being used. Therefore, Equation (8) was used to examine the metric accuracy.

$$\text{Accuracy} = \frac{\text{precise class segmentation}}{\text{complete test sets}} \text{ X } 100 \quad (8)$$

Additionally, Figure 12 elaborates the increased exactness rate for segmenting the brain tumour by the suggested TFFbU model. The accuracy of the training is about 0.99%. It demonstrates the proposed model's strong capacity to anticipate. To check the potential consequence of prediction accuracy and loss, the training loss and accuracy are also computed. Additionally, 80% of the images are utilized for training and 20% are used to verify the proposed algorithm's resilience.To determine the accuracy repeated in each iteration, the precision of the metrics was measured. The method used to assess the precision range, as seen in Equation (9),

$$precision = \frac{M_t}{M_t + N_p} \quad (9)$$

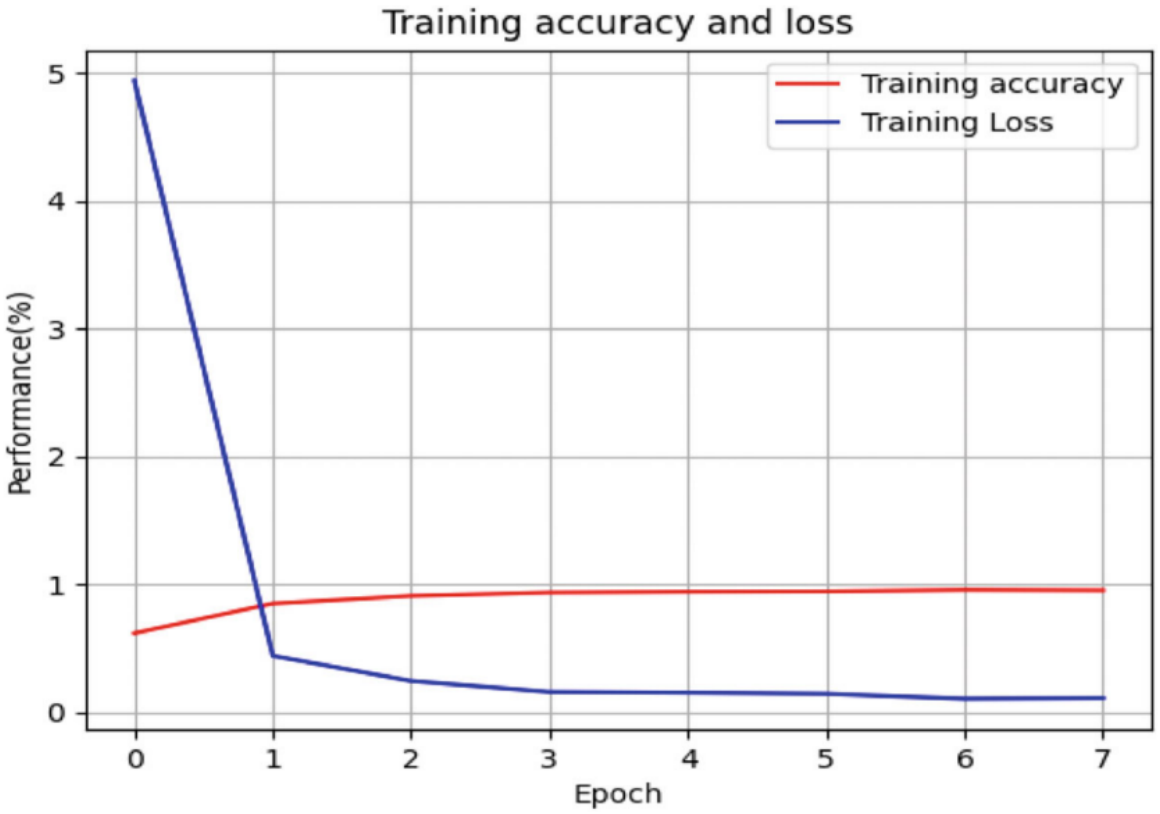

Fig 6 shows Training loss and Accuracy

where false positive is represented by the letters N_p, true negative by the letters N_t, true positive by the letters M_t, and false negative by the letters M_n. This accuracy parameter is also used to determine the segmentation's stability range.

Specificity and sensitivity

Measurement of the segmentation range from the segmented output is done using the term specificity. Additionally, matching the GTI results in the segmented output. The parameter specificity was therefore determined using Equation (10). Specificity is the measurement of the mean of segmentation accuracy, recall, and precision.

$$\text{specificity} = \frac{N_t}{N_t + N_p} \quad (10)$$

Sensitivity, which is also known as recall, was used to validate the results of the entire segmentation. Sensitivity is calculated as M_t divided by M_t and false negative M_n. Moreover, Equation (11) provides more information about this formula.

$$\text{sensitivity} = \frac{M_t}{M_t + M_n} \quad (11)$$

The effectiveness of any program may be determined by testing its sensitivity, accuracy, f-measure, and precision in addition to measuring the amount of time it takes to execute. In this section, a number of earlier models, such as the Fuzzy k-means model (FKM),[25] Optimized Laplacian (OL),[26] Component-Analysis, and Linear Discriminate Independent Model, were compared with the current models in order to calculate the improvement measure of the tumour segmentation system based on the current models. Supervised & Un-Supervised Learning (S-USL), and (CALDIM) [27]. [28]

It has been shown that the suggested method achieves a maximum accuracy of 99.99% and a recall rate of 99.75%. In contrast to the comparative traditional models, such as CALDIM, they have simultaneously obtained an accuracy

of 99.98% and a recall of 95.23%. Additionally, the technique OL recorded an accuracy of 98.76% and a recall rate of 96.38%. S-USC has achieved an accuracy of segmentation of 91% and a recall of 86%.

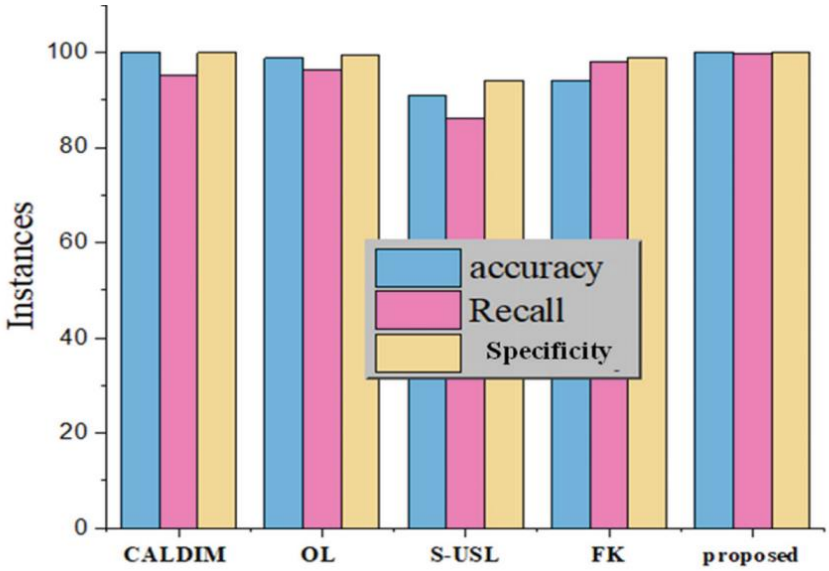

Fig 7 shows Assesment of Accuracy, recall and sensitivity

The approach FKM has produced segmentation accuracy of 94% and recall of 99.7%. Additionally, the created model's increased specificity score is 99.99%; earlier models like OL reported 99.4% specificity, FKM attained 99% specificity, CALDIM increased specificity by 99.97%, and the method S-USL increased specificity by 94%. Figure 7 provides a breakdown of the statistics for accuracy, recall, and specificity.

Precision was calculated to determine the segmentation rate's stability score. Additionally, it is described as the total number of precise segmentations across all trained datasets. The measured precision for the created TFFbU model is 99.6%; OL has achieved 98.2% precision, S-USL has produced 87% precision, and FKM has achieved 94% precision.

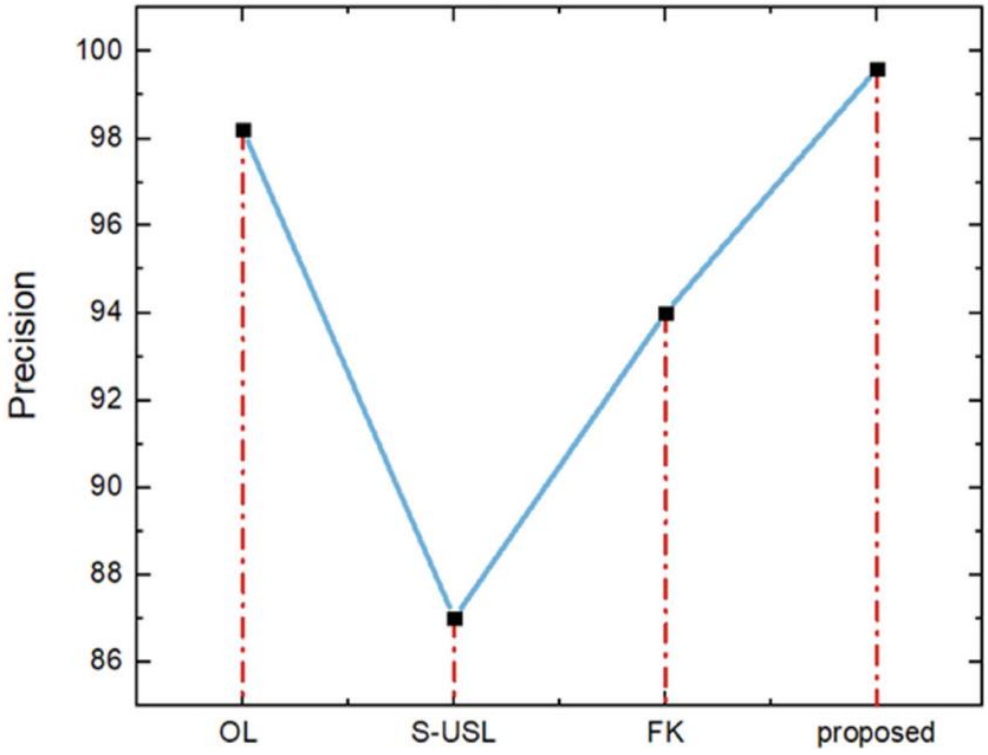

Fig 8 shows validation of precision

Dice and Jaccard

The primary parameter in the medical image processing system that is assessed to gauge the accuracy of segmentation is Dice and Jaccard. According to the medical applications, the segmentation score in this case was different. Here, rather than calculating F-value dice, an estimated value was used for B, the tumour region, and A, the features region in BT pictures. As a result, it provided the segmentation score and efficiency mean.

$$\text{Dice}(AB) = \frac{2(AB)}{(AB)+\frac{1}{2}\left(\frac{A}{B}\right)+\frac{1}{2}\left(\frac{B}{A}\right)} \quad (12)$$

$$\text{Jaccard} = \frac{(AB)}{(AB)+\left(\frac{A}{B}\right)+\left(\frac{B}{A}\right)} \quad (13)$$

Therefore, Equation (12) describes the dice formula, and Equation (13), the Jaccard formula. The loss score of various databases is used in this case to validate the metrics Dice and Jaccard. The trained dataset's foreground pixels are measured as dice.

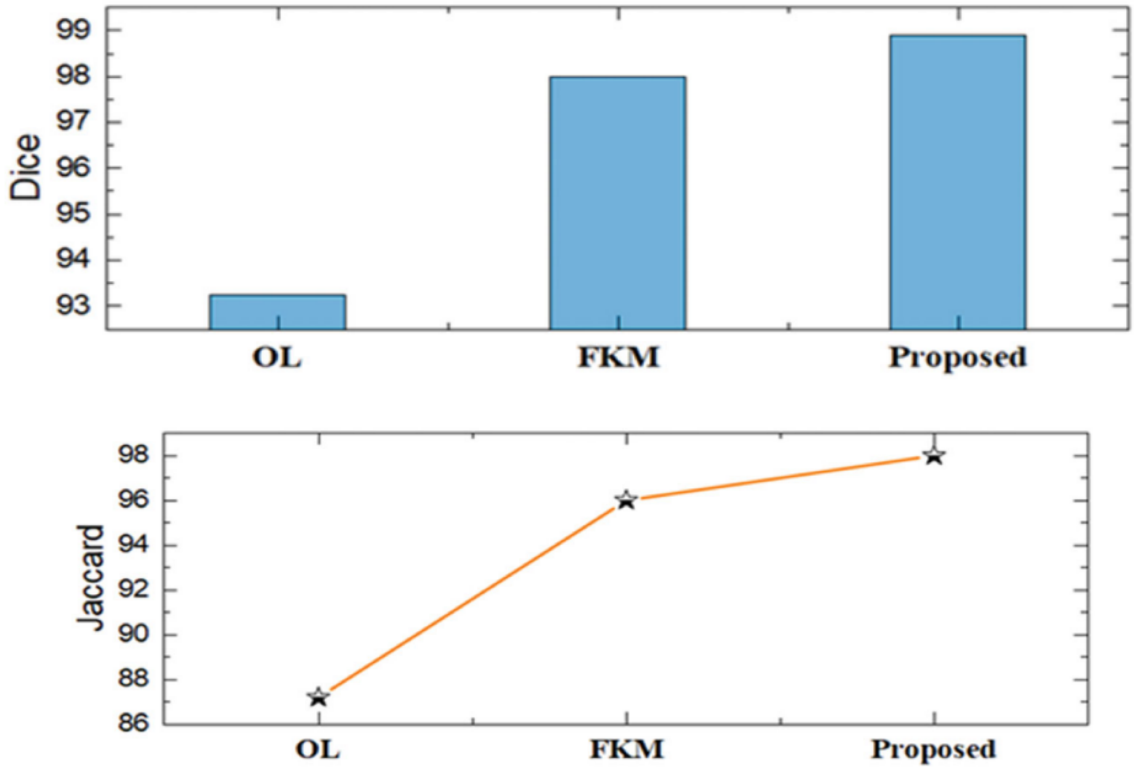

Fig 9 shows the performance of Dice and Jaccard

Table 1. overall performance Assesment

	Performance Assessment					
Method	Accuracy	Recall	Precision	Specificity	Dice	Jaccard
CALDIM[27]	99.98	95.23	-	99.97	-	-
OL[26]	98.76	96.38	98.2	99.4	93.2	87.2
S-USL[28]	91	86	87	94	-	-
FKM[25]	94	98	94	99	98	96
FFU	99.99	99.7	99.6	99.99	98.9	98
Proposed	99.98	99.8	99.7	99.8	99.1	98.5

Table 2 shows state of art Assesment

Authors	Methods	Merits	Limitations
Zhou et al.[17]	3D residual neural frameworks	The highest segmentation score was noted.	complicated timing
Lei et al.[18]	level-setting protocol	For segmentation, a wide range of accuracy was noted.	In order to process the intended model, more resources were required.
Khosravanian et al.[19]	Fuzzy with Boltzman	The function can be run with little execution time.	But designing is challenging.
Zhang et al.[20]	Deep features tumour extraction methods using different modalities	high accuracy rating in BT segmentation	The duration must be extended if the database is too large.
Saravanan et al.[27]	CALDIM	A noise reduction model was implemented in order to achieve the best segmentation results.	However, a variety of complexity scores have been reported.
Saman and Narayanan[26]	OL	The highest segmentation exactness score was attained by it.	However, it is a manual procedure and not an automated one.
Al-Saffar et al.[28]	S-USL	The difficulty in evaluating the MRI BT data was precisely confirmed.	The lengthy time required to complete the process
Pitchai et al.[25]	FKM	With the assistance of the DL model, it has achieved the best segmentation results.	However, more resources were required to complete it.
Proposed	TFFbU	TFF fitness is combined with the UNet dense layer in this TFFbU model to provide superior segmentation outcomes. Additionally, the output was validated and the results were compared to various illness brain tumour images.	

5. Discussion

In each investigation, a number of factors were examined with varying data volumes; the reported FFbU achieved the best results for separating the BT from the trained MRI data. Table 1 summarizes the overall stellar outcomes.Table 2 discusses the current state of the art for the related and contrasted model. Additionally, each method's advantages and disadvantages were examined.and a report." The proposed TFFbU model resolves issues that have been reported utilizing the current techniques.

Additionally, the projected TFFbU has only used a maximum of 10 seconds to segment the BT from the training MRI. However, older techniques like the Convolutional model29 needed a maximum of 64s to complete the segmentation process, while CALDIM[27] only needed17s. Therefore, taking into account that the suggested TFFbU technique has produced the most amazing results in a short amount of time. Hence,The suggested TFFbU model can monitor and segregate the BT from training MRI data in the medical industry.

6. Conclusion

For various brain tumour segmentation, the FFbU model has been used in the current study. In order to get remarkable results, the fruit fly fitness solution is enhanced in the UNet classification layer. Finally, a novel TFFbU's robustness was evaluated using a variety of measures, including dice, Jaccard, recall, precision, accuracy, recall, and specificity. The predicted FFbU model has got the better result in all metrics validated by resulting in 98.5% Jaccard, 99.1% Dice, 99.8% accuracy, and 99.8% specificity. Additionally, the segmentation process has a stated maximum running time of 12 s, which is far faster than traditional techniques. By contrasting the

projected FFbU with other models, the segmentation exactness score has increased up to 3% and the execution time has decreased by up to 7 s. The hybrid DL mechanism combined with the heuristic mechanism will, in the future, generate results that are superior to those produced by this present work in designing as a result of the incorporation of the segmentation error detection mechanism.

References

[1] Das S, Bose S, Nayak GK, Satapathy SC, Saxena S. Brain tumor segmentation and overall survival period prediction in glioblastoma multiforme using radiomic features. Concurr Comput Pract Exp. 2021;e6501. doi:10.1002/cpe.6501

[2] Xie X, Li L, Lian S, Chen S, Luo Z. SERU: a cascaded SE-ResNeXT U-net for kidney and tumor segmentation. Concurr Comput Pract Exp. 2020;32(14):e5738. doi:10.1002/cpe.5738

[3] Thiruvenkadam K, Nagarajan K, Padmanaban S. An automatic self-initialized clustering method for brain tissue segmentation and pathology detection from magnetic resonance human head scans with graphics processing unit machine.Concurr Comput Pract Exp. 2021;33(6):e6084. doi:10.1002/cpe.6084

[4] Zhang D, Huang G, Zhang Q, Han J,Wang Y, Yu Y. Exploring task structure for brain tumor segmentation from multi-modalityMR images. IEEE Trans Image Process. 2020;29:9032-9043. doi:10.1109/TIP.2020.3023609

[5] Naser MA, Deen MJ. Brain tumor segmentation and grading of lower-grade glioma using deep learning in MRI images. Comput Biol Med. 2020;121:103758. doi:10.1016/j.compbiomed.2020.103758

[6] Di Ieva A, Russo C, Liu S, et al. Application of deep learning for automatic segmentation of brain tumors on magnetic resonance imaging: a heuristic approach in the clinical scenario. Neuroradiology. 2021;63:1-10. doi:10.1007/s00234-021-02649-3

[7] Tran DH, Winkler-Schwartz A, TuznikM, et al. Quantitation of tissue resection using a brain tumor model and MRI Imaging. World surgeon 2021;148:e326-e339. doi:10.1016/j.wneu.2020.12.141

[8] Menze B, Isensee F, Wiest R, et al. Analyzing magnetic resonance imaging data from glioma patients using deep learning. Comput Med Imaging Graph. 2021;88:101828. doi:10.1016/j.compmedimag.2020.101828

[9] Mohammed E, Hassaan M, Amin S, Ebied HM. Brain tumor segmentation: a comparative analysis. In: The International Conference on Artificial Intelligence and Computer Vision, Springer, Cham; 2021. doi:10.1007/978-3-030-76346-6_46

[10] Lin F,Wu Q, Liu J,Wang D, Kong X. Path aggregation U-net model for brain tumor segmentation. Multimed Tools Appl. 2021;80(15):22951-22964. doi:10. 1007/s11042-020-08795-9

[11] Alhassan AM, Zainon WMNW. Brain tumor classification in magnetic resonance image using hard swish-based RELU activation function-convolutional neural network. Neural Comput Appl. 2021;33:9075-9087. doi:10.1007/s00521-020-05671-3

[12] Bacanin N, Bezdan T, Venkatachalam K, Al-Turjman F. Optimized convolutional neural network by firefly algorithm for magnetic resonance image classification of glioma brain tumor grade. J Real Time Image Process. 2021;18:1085-1098. doi:10.1007/s11554-021-01106-x

[13] Biswas A, Bhattacharya P,Maity SP, Banik R. Data augmentation for improved brain tumor segmentation. IETE J Res. 2021;1-11. doi:10.1080/03772063. 2021.1905562 BODA ET AL. 17 of 17

[14] Budati AK, Katta RB. An automated brain tumor detection and classification from MRI images using machine learning techniques with IoT. Environ Dev Sustain. 2021;1-15. doi:10.1007/s10668-021-01861-8

[15] Zhou T, Canu S, Vera P, Ruan S. Latent correlation representation learning for brain tumor segmentation with missing MRI modalities. IEEE Trans Image Process. 2021;30:4263-4274. doi:10.1109/TIP.2021.3070752

[16] Chikhalikar AM, Dharwadkar NV.Model for enhancement and segmentation of magnetic resonance images for brain tumor classification. Pattern Recogn Image Anal. 2021;31(1):49-59. doi:10.1134/S1054661821010065

[17] Zhou X, Li X, Hu K, Zhang Y, Chen Z, Gao X. ERV-net: an efficient 3D residual neural network for brain tumor segmentation. Expert Syst Appl. 2021;170:114566. doi:10.1016/j.eswa.2021.114566

[18] Lei X, Yu X, Chi J, Wang Y, Zhang J, Wu C. Brain tumor segmentation in MR images using a sparse constrained level set algorithm. Expert Syst Appl. 2021;168:114262. doi:10.1016/j.eswa.2020.114262

[19] Khosravanian A, Rahmanimanesh M, Keshavarzi P, Mozaffari S. Fast level set method for glioma brain tumor segmentation based on superpixel fuzzy clustering and lattice boltzmann method. Comput Methods Programs Biomed. 2021;198:105809. doi:10.1016/j.cmpb.2020.105809

[20] Zhang D, Huang G, Zhang Q, Han J, Han J, Yu Y. Cross-modality deep feature learning for brain tumor segmentation. Pattern Recogn. 2021;110:107562. doi:10.1016/j.patcog.2020.107562

[21] Tiwari A, Srivastava S, Pant M. Brain tumor segmentation and classification from magnetic resonance images: review of selected methods from 2014 to 2019. Pattern Recogn Lett. 2020;131:244-260. doi:10.1016/j.patrec.2019.11.020

[22] Selvathi D. Brain tissues segmentation inmagnetic resonance imaging for the diagnosis of brain disorders using a convolutional neural network.Handbook of Decision Support Systems for Neurological Disorders. Academic Press; 2021:167-186. doi:10.1016/B978-0-12-822271-3.00014-1

[23] Fan Y, Wang P, Heidari AA, et al. Rationalized fruit fly optimization with sine cosine algorithm: a comprehensive analysis. Expert Syst Appl. 2020;157:113486. doi:10.1016/j.eswa.2020.113486

[24] ShuvoMB,Ahommed R, Reza S, HashemMMA.CNL-UNet: a novel lightweight deep learning architecture formultimodal biomedical image segmentation with false output suppression. Biomed Signal Process Control. 2021;70:102959. doi:10.1016/j.bspc.2021.102959

[25] Pitchai R, Supraja P, Victoria AH, Madhavi M. Brain tumor segmentation using deep learning and fuzzy K-means clustering for magnetic resonance images. Neural Process Lett. 2021;53(4):2519-2532. doi:10.1007/s11063-020-10326-4

[26] Saman S, Narayanan SJ. Active contour model driven by optimized energy functionals for MR brain tumor segmentation with intensity inhomogeneity correction. Multimed Tools Appl. 2021;80(14):21925-21954. doi:10.1007/s11042-021-10738-x

[27] Saravanan S, Karthigaivel R, Magudeeswaran V. A brain tumor image segmentation technique in image processing using ICA-LDA algorithm with ARHE model. J Ambient Intell Hum Comput. 2021;12(5):4727-4735. doi:10.1007/s12652-020-01875-6

[28] Al-Saffar ZA, Yildirim T. A hybrid approach based on multiple eigenvalues selection (MES) for the automated grading of a brain tumor using MRI. Comput Methods Programs Biomed. 2021;201:105945. doi:10.1016/j.cmpb.2021.105945

[29] Kesav N, Jibukumar MG. Efficient and low complex architecture for detection and classification of brain tumor using RCNN with two channel CNN. J King Saud Univ- Comput Inf Sci. 2021. doi:10.1016/j.jksuci.2021.05.008

[30] Fu, J. ., & Saad, N. H. M. . (2023). Cross Border E-Commerce Uses Blockchain Technology to Solve Payment Risks. International Journal on Recent and Innovation Trends in Computing and Communication, 11(3s), 205–215. https://doi.org/10.17762/ijritcc.v11i3s.6182

[31] Johansson Anna, Maria Jansen, Anna Wagner, Anna Fischer, Maria Esposito. Machine Learning Techniques to Improve Learning Analytics. Kuwait Journal of Machine Learning, 2(2). Retrieved from http://kuwaitjournals.com/index.php/kjml/article/view/189

[32] Anand, R., Ahamad, S., Veeraiah, V., Janardan, S. K., Dhabliya, D., Sindhwani, N., & Gupta, A. (2023). Optimizing 6G wireless network security for effective communication. Innovative smart materials used in wireless communication technology (pp. 1-20) doi:10.4018/978-1-6684-7000-8.ch001 Retrieved from www.scopus.com